

## Crossover from low-dimensional to three-dimensional ferromagnetism in $\text{CePd}_{1-x}\text{Pt}_x\text{Sb}$ alloys

D. T. Adroja, J. G. M. Armitage, and P. C. Riedi

*School of Physics and Astronomy, University of St. Andrews, Fife, KY16 9SS, United Kingdom*

M. R. Lees and O. A. Petrenko

*Department of Physics, Warwick University, Coventry, CV4 7AL, United Kingdom*

(Received 26 July 1999)

The hexagonal material  $\text{CePdSb}$  exhibits low-dimensional ferromagnetism with  $T_c = 17.5$ , while isostructural  $\text{CePtSb}$  shows normal three-dimensional ferromagnetism with  $T_c = 4.8$  K. To understand the low-dimensional ferromagnetic ordering of  $\text{CePdSb}$  we have investigated  $\text{CePd}_{1-x}\text{Pt}_x\text{Sb}$  alloys, using ac susceptibility, heat capacity, thermal expansion, and zero-field spin-echo NMR measurements. The ac susceptibility shows that the  $T_c$  of the Pd-rich alloys is higher than that expected from a linear extrapolation of the Pt-rich alloys. The heat capacity shows a smooth crossover from the anomalous ( $x \leq 0.4$ ) to normal ( $x \geq 0.6$ ) ferromagnetic behavior with increasing Pt concentration. Thermal expansion results agree with the heat-capacity data for the alloys that are either Pd rich ( $x \leq 0.2$ ) or Pt rich ( $x \geq 0.8$ ). However, the thermal expansion shows anomalous behavior for the alloys  $x = 0.4$  and  $0.6$ , in the composition range where the heat capacity exhibits the crossover behavior. From the heat capacity and ac susceptibility measurements a phase diagram, temperature vs  $x$ , for  $\text{CePd}_{1-x}\text{Pt}_x\text{Sb}$  alloys has been proposed. Low power zero-field Sb spin-echo NMR studies show well-defined quadrupole split NMR spectra in both  $\text{CePdSb}$  and  $\text{CePtSb}$ , confirming the ferromagnetic ground state. Only a very broad NMR signal has been observed in the substituted alloys of  $\text{CePd}_{1-x}\text{Pt}_x\text{Sb}$  ( $0.1 \leq x \leq 0.8$ ) because of the differences between the quadrupole splitting of  $\text{CePtSb}$  and  $\text{CePdSb}$ . The internal field at the Sb nucleus at low temperatures for  $\text{CePtSb}$ ( $\text{CePdSb}$ ) is  $+2.3$  T ( $+2.8$  T) and the quadrupole splitting 8.5 and 5.1 MHz (3.8 and 2.3 MHz) for  $^{121}\text{Sb}$  and  $^{123}\text{Sb}$ , respectively.

### I. INTRODUCTION

There has been considerable interest recently in the ternary equiatomic compounds of the type  $\text{CeTX}$ , where  $T$  is a transition metal atom and  $X$  is a metalloid atom. Reports of the magnetic and transport properties reveal the presence of many interesting ground states, namely, valence fluctuation, heavy fermion, Kondo-insulator, and unusual ferromagnetism.<sup>1-5</sup> The stability of the ground state depends on the competition between the on-site single-ion Kondo energy,  $T_K$ , and the intersite RKKY (Ruderman-Kittel-Kasuya-Yosida) energy,  $T_{\text{RKKY}}: T_K \propto \exp[-1/J_{sf}\rho(E_F)]$  and  $T_{\text{RKKY}} \propto [J_{sf}\rho(E_F)]^2$ , where  $J_{sf}$  is the  $4f$  and conduction electrons coupling constant and  $\rho(E_F)$  is the density of states of conduction electrons at the Fermi energy,  $E_F$ .<sup>6</sup> The former stabilizes the nonmagnetic ground state, while the latter stabilizes the magnetic ground state. Both effects originate from the antiferromagnetic  $s$ - $f$  exchange coupling  $J_{sf}$ , which depends on the hybridization between conduction and localized  $4f$  states and the position of the  $4f$  state relative to the Fermi energy.<sup>7</sup>

Usually Kondo lattices exhibit an antiferromagnetic ground state at low temperatures, but a handful of compounds have been reported to have a ferromagnetic ground state.<sup>4,8</sup> Among them are the hexagonal compounds  $\text{CeTSb}$  with  $T = \text{Ni}$ , Pd, and Pt that order ferromagnetically at 4 K, 17.5 K, and 4.8 K, respectively.<sup>4,9,10</sup> The magnetic ordering temperature of  $\text{CePdSb}$  is rather high compared to other members of the family and also compared to other isostructural  $\text{RPdSb}$  ( $R = \text{Nd}$ , Sm, Eu, and Gd) compounds, all of which order antiferromagnetically.<sup>11</sup> Using de Gennes scaling and  $T_N = 15.5$  K of  $\text{GdPdSb}$ , one would expect the ordering temperature of  $\text{CePdSb}$  to be 91 times smaller than that

of  $\text{GdPdSb}$ , which is not the case. This suggests that the magnetic ordering temperature of  $\text{CePdSb}$  is anomalous. The heat capacity, thermal expansion, spontaneous magnetization, and small angle neutron-scattering studies show unusual behavior, which makes  $\text{CePdSb}$  the most interesting compound among the family.<sup>12-17</sup> The heat capacity and thermal expansion of single crystal samples exhibit a very weak anomaly at  $T_c (= 17.5$  K), but rather a broad Schottky-like peak centered at 10 K. The temperature dependence of the spontaneous magnetization exhibits a point of inflexion near 10 K, and a rather slow approach to the region of the Curie point.<sup>16</sup> From the low value of the electronic specific heat coefficient,  $\gamma = 11$  mJ/mole-K<sup>2</sup> and the full magnetic entropy of the doublet ground state at  $T_c$ , it has been claimed that the Kondo effect does not exist in  $\text{CePdSb}$ .<sup>12</sup> This view is supported by the temperature independent and strong  $q$ -dependent quasielastic linewidth of neutron scattering in the paramagnetic state.<sup>16</sup> On the other hand the pressure dependence of  $T_c$  of  $\text{CePdSb}$  exhibits an asymmetric maximum ( $T_c = 31$  K at 10 Gpa) in the  $T_c$  vs pressure curve.<sup>18</sup> This behavior has been explained quite well by the Doniach phase diagram, which considers the competition between RKKY and Kondo interactions for the one-dimensional Kondo-necklace model.<sup>7</sup> These results show that the existence of the Kondo effect in  $\text{CePdSb}$  is open to debate at present. Other interesting behavior has been observed in the small angle neutron scattering (SANS) measurements on a single crystal of  $\text{CePdSb}$ .<sup>17</sup> SANS reveals that the correlation length ( $\xi$ ) is finite between  $T_c$  and 8 K ( $\xi = 84 - 417$  Å in the  $bc$  plane and 40 Å in the  $ab$  plane) and diverges to infinity below 8 K (10 K) in the  $bc$  plane (in the  $ab$  plane). These results along with the heat capacity, magnetization, and thermal expansion indicate a low-dimensional ferromagnetic ordering between

$T_c = 17.5$  K and 10 K in CePdSb.

On the other hand isostructural CePtSb shows normal three-dimensional (3D) ferromagnetic behavior below 5 K with the heat capacity exhibiting a sharp peak at  $T_c$ . Inelastic neutron-scattering studies show well-defined crystal field excitations in both the compounds at energies of 26.5 (25.2) and 32.1 (29.1) meV in CePdSb (CePtSb).<sup>9</sup> The values of the crystal field (CF) parameters are  $B_2^0 = 1.36$  (0.74),  $B_4^0 = -0.05$  (-0.05), and  $B_4^3 = 0.86$  (1.28) meV for CePdSb (CePtSb).<sup>9</sup> These sets of CF parameters give a large anisotropy between the basal plane and  $c$  axis with the magnetic moment lying in the  $ab$  plane. This prediction agrees well with the magnetization measurements on single crystals of CePdSb and CePtSb.<sup>14</sup> The susceptibility analysis suggests that the ferromagnetic exchange interaction along the  $c$  axis is much stronger in CePdSb ( $\lambda_c = 100$  emu/mole) than in CePtSb ( $\lambda_c = 40$  emu/mole).<sup>14</sup> It is to be noted that the linewidth of the second CF excitation in CePdSb is much larger than that of the first CF excitation and also compared with linewidth of the CF excitations in CePtSb. This may be due to the symmetry dependence of the hybridization matrix element of the CF levels with the conduction electrons, especially with the  $d$  band of the Pd or  $p$  band of the Sb. This raises the question of the existence of the Kondo effect in CePdSb at high temperatures coming from the second excited CF level. This type of behavior has been observed in the low-carrier density compound CeSb, where the Kondo effect arises from the excited CF level,  $\Gamma_8$ , while the ground-state  $\Gamma_7$ , does not take part in the Kondo effect.<sup>19</sup> The resistivity of CePdSb and CePtSb exhibits quasi-two-dimensional behavior.<sup>14</sup> The absolute value of the Hall-coefficient of both the compounds is much larger than that of a typical semimetal suggesting that CePdSb and CePtSb belong to the low-carrier density systems.<sup>14</sup>

In order to understand the low-dimensional ferromagnetic ordering of CePdSb, compared with normal 3D ferromagnetic ordering of CePtSb, we have synthesized CePd<sub>1-x</sub>Pt<sub>x</sub>Sb alloys and investigated them using x-ray diffraction, ac susceptibility, heat capacity, thermal expansion, magnetostriction, and zero-field Sb, NMR measurements. The results of these studies are presented in this paper.

## II. EXPERIMENTAL DETAILS

The polycrystalline samples of CePd<sub>1-x</sub>Pt<sub>x</sub>Sb ( $x = 0$  to 1) were prepared by the usual arc-melting of stoichiometric amounts of the constituents elements (purity 4N for Ce, Pd, Pt, and 6N for Sb) on a water-cooled hearth in an Ar atmosphere. Due to the volatile nature of Sb, about 2 wt% excess of Sb was added before the first melting, which compensated for Sb losses. Powder x-ray diffraction (XRD) studies were carried out using a Philips diffractometer with Cu- $K_\alpha$  radiation at room temperature. The complex ac susceptibility was measured in a field of 5 G between 3 and 30 K at a frequency of 525 Hz using the mutual-inductance method with a lock-in amplifier. The heat-capacity measurements were performed using the standard heat-pulse method between 2 K and 25 K, at the University of Warwick. Thermal expansion measurements were carried out in a parallel plate capacitance cell that had been calibrated using the known thermal expan-

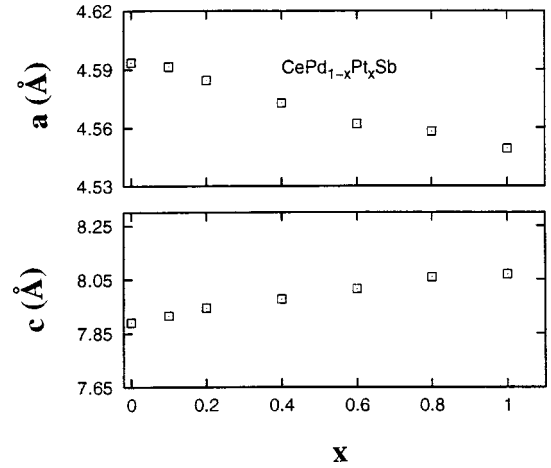


FIG. 1. Lattice parameters,  $a$  and  $c$ , vs Pt concentration,  $x$  for CePd<sub>1-x</sub>Pt<sub>x</sub>Sb alloys. The error bars are same size as the symbols.

sivity of Si. The relative accuracy of the method was,  $\Delta/I \approx 1 \times 10^{-7}$ .

The  $^{121}\text{Sb}$  ( $\gamma_n/2\pi = 10.19$  MHz  $T^{-1}$ ,  $I = 5/2$ ) and  $^{123}\text{Sb}$  ( $\gamma_n/2\pi = 5.52$  MHz  $T^{-1}$ ,  $I = 7/2$ ) NMR measurements were carried out using a zero-field spin-echo NMR spectrometer in a swept frequency phase-coherent mode, with the sample in a low- $Q$  untuned coil, at 4 K and 1.5 K.<sup>20</sup> The natural abundance of  $^{121}\text{Sb}$  ( $^{123}\text{Sb}$ ) is 57.25 (42.75)%. Spin echoes were observed at low applied RF power, due to the enhancement of the RF field by domain wall motion.

## III. RESULTS AND DISCUSSION

### A. XRD and ac susceptibility

Our XRD studies show that all the alloys are single-phase materials and crystallize in the hexagonal GaGeLi-type structure with space group  $P6_3mc$ .<sup>21</sup> The hexagonal GaGeLi-type structure is an ordered structure in which there exist three different crystallographic sites for the Ce, Pd(Pt), and Sb atoms. The crystallographic ordering between Pt and Sb sites in CePtSb has been confirmed through the Rietveld refinement of the powder neutron diffraction data.<sup>9</sup> Due to the ordering between Pd(Pt) and Sb, the point symmetry of the Ce site reduces from sixfold to threefold, which gives an extra term,  $B_4^3 O_4^3$ , in the crystal-field Hamiltonian. The unit cell of CeTSb compounds can be viewed as two-dimensional hexagonal layers of Ce atoms, sandwiched by the nets of  $T$  and Sb atoms along the  $c$  axis. Alternatively this structure can also be viewed as chains of Ce atoms along the  $c$  axis separated by the zigzag chains of  $T$  and Sb atoms. The lattice parameters,  $a$  and  $c$ , obtained from the positions of the diffraction peaks ( $10^\circ \leq 2\theta \leq 90^\circ$ ) are plotted as a function of Pt composition in Fig. 1. It can be seen from Fig. 1 that  $a$  decreases almost linearly with  $x$ , with a rate of  $da/dx \approx -0.045$  Å, while  $c$  increases linearly with  $x$ , with a rate of  $dc/dx \approx 0.174$  Å,  $a = 4.593(5)$  Å:  $c = 7.890(7)$  Å for CePdSb and  $a = 4.549(8)$  Å,  $c = 8.069(4)$  Å for CePtSb. In the hexagonal GaGeLi-type structure the shortest Ce-Ce distance is  $c/2$  along the  $c$  axis. This indicates that going from CePdSb to CePtSb the nearest-neighbor Ce-Ce distance along the  $c$  axis is increased, which may effect the magnetic properties of the Ce ions. The observed volume change be-

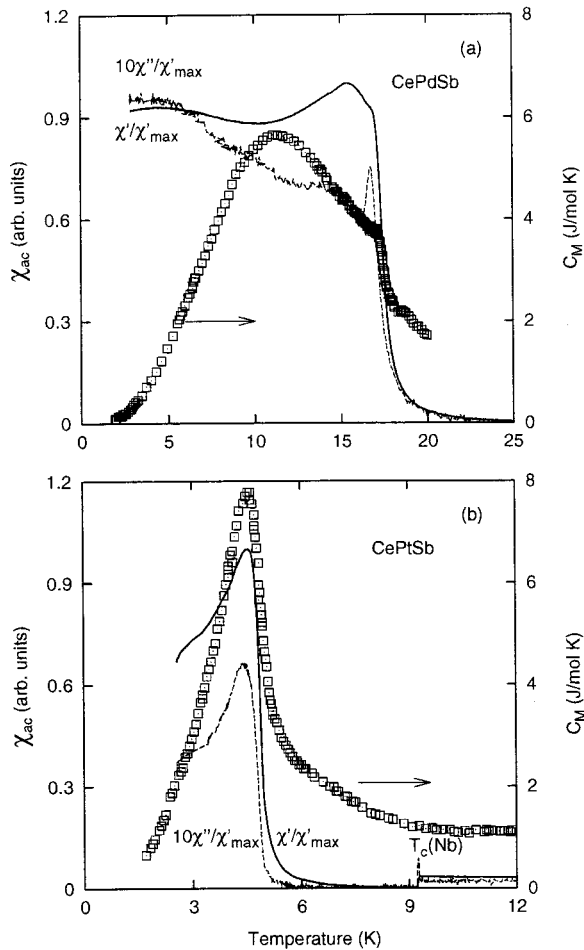


FIG. 2. Inductive,  $\chi'(T)$  and dissipative,  $\chi''(T)$  components of the ac susceptibility normalized to the maximum of  $\chi'(T)$  between 3 K and 25 K. The temperature-dependent heat-capacity data (from Ref. 13) is plotted on the secondary y-axis for comparison. The peak at 9.2 K in  $\chi''(T)$  in Fig. 2(b) is from the Nb used as temperature calibration.

tween CePdSb and CePtSb at room temperature is,  $\Delta V/V \approx 0.31\%$ . In the isostructural and isoelectronic ferromagnetic compounds CeTSb ( $T = \text{Ni, Pd and Pt}$ ), the shortest Ce-Ce distance is in CePdSb (3.945 Å), compared to that in CePtSb (4.035 Å) and CeNiSb (4.151 Å). This is greater than the Hill limit of 3.25–3.4 Å, the minimum distance for the direct overlap between  $f$ -wave functions to occur, which suggests that the indirect RKKY interaction mediated through conduction electrons is responsible for the magnetic ordering of CeTSb compounds. However, the fact that in these compounds the Ce-Ce distance is shortest for CePdSb suggests that there may also be a short-range contribution to the magnetic exchange leading to the high value of  $T_c$  for CePdSb.

The  $T_c$  of  $\text{CePd}_{1-x}\text{Pt}_x\text{Sb}$  alloys was determined from the low-field (5G) ac susceptibility,  $\chi_{ac}$  measurements. Figure 2 shows typical  $\chi_{ac}(T)$  signals, inductive ( $\chi'$ ) and dissipative ( $\chi''$ ), from CePdSb and CePtSb. For comparison purposes the heat-capacity results are also plotted on the secondary y axis. For CePdSb both  $\chi'(T)$  and  $\chi''(T)$  exhibit a sharp rise below 19 K, followed by a peak at 15.4 K and 16.86 K, respectively, which is due to the ferromagnetic ordering of the Ce moments. It was shown that the peak position is frequency dependent, which has been attributed to non-trivial

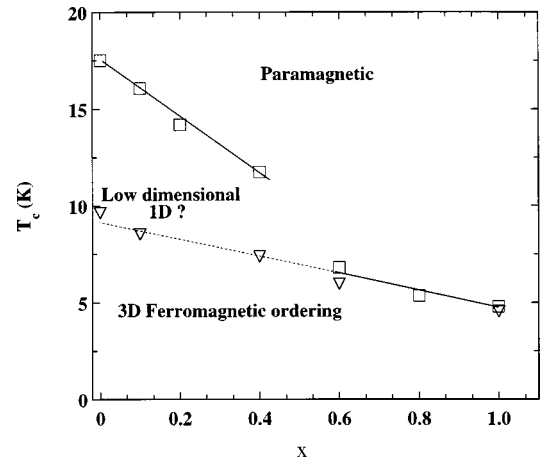


FIG. 3. Phase diagram of  $\text{CePd}_{1-x}\text{Pt}_x\text{Sb}$  ( $0 \leq x \leq 1$ ) alloys obtained from the heat capacity and ac susceptibility measurements. The ordering temperature,  $T_c$  (estimated from ac susceptibility) as a function of Pt concentration (squares). The peak position in the heat capacity as a function of  $x$  (triangles). The solid and dotted lines are guides to the eye.

dynamics of the interacting magnetic moments.<sup>12</sup> The peak in the  $\chi''(T)$  is sharper than that in  $\chi'(T)$ , which is due to the maximum losses near  $T_c$ . Further,  $\chi'(T)$  exhibits a weak and broad peak at 5 K, compared with the clear peak at 6 K observed in Ref. 12. The origin of this peak is not clear at present, but may be related with the onset of the zero-frequency modes at 6 K ( $T \leq 6$  K, no quasi-elastic response) in the inelastic neutron-scattering study.<sup>16</sup> The midpoint of the rise of  $\chi'(T)$  gives  $T_c = 17.5$  K for CePdSb, which is in agreement with the heat-capacity data on single-crystal CePdSb [see Fig. 2(a)]. The  $\chi'(T)$  and  $\chi''(T)$  of CePtSb exhibit a sharp rise below 6 K followed by a peak at 4.6 and 4.5 K, respectively. The peak position in  $\chi'(T)$  agrees well with that observed in the heat capacity [see Fig. 2(b)], while the peak in  $\chi''(T)$  is at a slightly lower temperature than the  $T_c$ . Further, it is to be noted that the heat capacity starts rising well above  $T_c$ , which may suggest the presence of magnetic fluctuations above  $T_c$ . As  $\chi_{ac}(T)$  does not show a clear anomaly above  $T_c$ , the implication is that the fluctuations above  $T_c$  are suppressed by a measuring field of 5 G. A very similar response in  $\chi_{ac}$  was observed for other alloys with  $x = 0.1$  to 0.8.

Figure 3 shows the ferromagnetic transition temperature,  $T_c$  of  $\text{CePd}_{1-x}\text{Pt}_x\text{Sb}$  alloys as a function of Pt composition  $x$ . The  $T_c$  was determined from the midpoint of the rise of  $\chi'(T)$ . The  $T_c$  vs  $x$  plot exhibits linear behavior in two different regions. For Pd-rich alloys  $T_c$  drops with a rate of  $dT_c/dx = -14.7$  K, while for Pt-rich alloys the rate is  $dT_c/dx = -4.2$  K. As CePtSb exhibits normal ferromagnetic behavior, we estimated the hypothetical  $T_c$  of CePdSb (in its normal state, i.e., without anomalous behavior) by extrapolating the linear behavior from Pt-rich alloys (dotted line in Fig. 3). This gives a  $T_c = 9.1$  K of CePdSb, which is almost half the value of the true experimental  $T_c = 17.5$  K, but close to the anomalous behavior observed in the heat capacity (9.7 K), thermal expansion (10 K), and small angle neutron-scattering (8–12 K). This suggests that only below 10 K does the magnetic state of CePdSb show three-dimensional order, while between  $T_c$  and 10 K an unusual magnetic state exists.

This unusual state has been attributed to the low-dimensional magnetic ordering.<sup>12,14</sup> Further, it is to be noted a large value of  $dT_c/dx = -75$  K has been observed in CePdSb, when 10% of Pd is replaced by Rh.<sup>22</sup> Rh has one electron less than Pd, while Pt is isoelectronic to Pd. This may imply that the driving forces for the large change in  $dT_c/dx$  for Rh substituted alloys are both volume/lattice parameter and electronic concentration effects, while the  $T_c$  changes in Pt substituted alloys are mainly due to volume/lattice parameter effect, which may in turn change the hybridization and hence the magnetic exchange as  $J_{sf} = -|V_{sf}|/E_{ex}$ , where  $V_{sf}$  is the hybridization strength and  $E_{ex}$  is the energy difference between the  $4f$  level and Fermi level.

### B. Heat capacity

Figures 4(a)–(e) show the magnetic contribution of the heat capacity,  $C_M$  of  $\text{CePd}_{1-x}\text{Pt}_x\text{Sb}$  alloys as a function of temperature. The heat-capacity data of CePdSb (both polycrystalline and single crystalline) and CePtSb are taken from Refs. 12 and 13 for completeness. The magnetic contribution to the heat capacity of all the alloys, except  $x = 1$ , was obtained by subtracting the heat capacity of the reference compound LaAgGe as used in Ref. 12. For CePtSb,  $C_M$  was obtained by subtracting the heat capacity of LaPtSb.<sup>13</sup> Before discussing the heat-capacity behavior of the Pt-substituted alloys, we will first recapitulate the heat-capacity behavior of CePdSb as discussed in Refs. 12–14. The heat capacity of the polycrystalline CePdSb increases gradually with decreasing temperature from 25 K and exhibits a broad maximum at 9.7 K, without any clear sign of anomaly at  $T_c = 17.5$  K. On the other hand for the single crystal sample the heat capacity exhibits a sharp jump at  $T_c$  followed by a broad maximum at 10.5 K. A very similar behavior has been reported in the thermal expansion studies.<sup>15</sup> Below 8 K the heat capacity of both the samples exhibits a behavior,  $C_M(T) \propto AT^n \exp(-\Delta/T)$ , where  $\Delta$  is an energy gap in the spin-wave spectrum and  $n = 3/2$  for a ferromagnetic ground state, while  $n = 3$  for an antiferromagnetic ground state. The reported value of  $\Delta$  is 4.5 K (with  $n = 1.7$ ) and 6.33 K (with  $n = 1.5$ ), for the polycrystalline and single-crystalline samples, respectively.<sup>12,14</sup> Further, the heat capacity of the polycrystalline sample has been fitted to a  $T^{-2}$  law between  $T \geq 14$  K and 20 K, which is characteristic of a magnetic chain. This behavior has been interpreted as due to the low-dimensional ordering (ordering along  $c$ -axis chain) of the Ce moments between  $T_c$  and 10 K.<sup>12,14</sup> The value of the magnetic entropy at 10 K is about  $0.5R \ln(2)$  and reaches a value of  $1.2R \ln(2)$  at 25 K, which agrees with the entropy of a doublet crystal-field ground state.

The heat-capacity results for the Pt-substituted alloys are summarized in Figs. 4(a)–(e). The dramatic change in the heat-capacity behavior is observed with Pt composition between  $x = 0.4$  and  $x = 0.6$  alloys: the anomalous peak observed in CePdSb still exists up to  $x = 0.4$  composition, on the other hand for the  $x = 0.6$  alloy the heat capacity exhibits a sharp peak as predicted in the mean-field theory for the second-order phase transition. The heat-capacity behavior of the  $x = 0.6$  alloy is similar to that observed in CePtSb compound, see Fig. 4(e).  $C_M(T)$  of the  $x = 0.1$  alloy exhibits a small jump at 15.9 K, which coincides with the sharp rise in

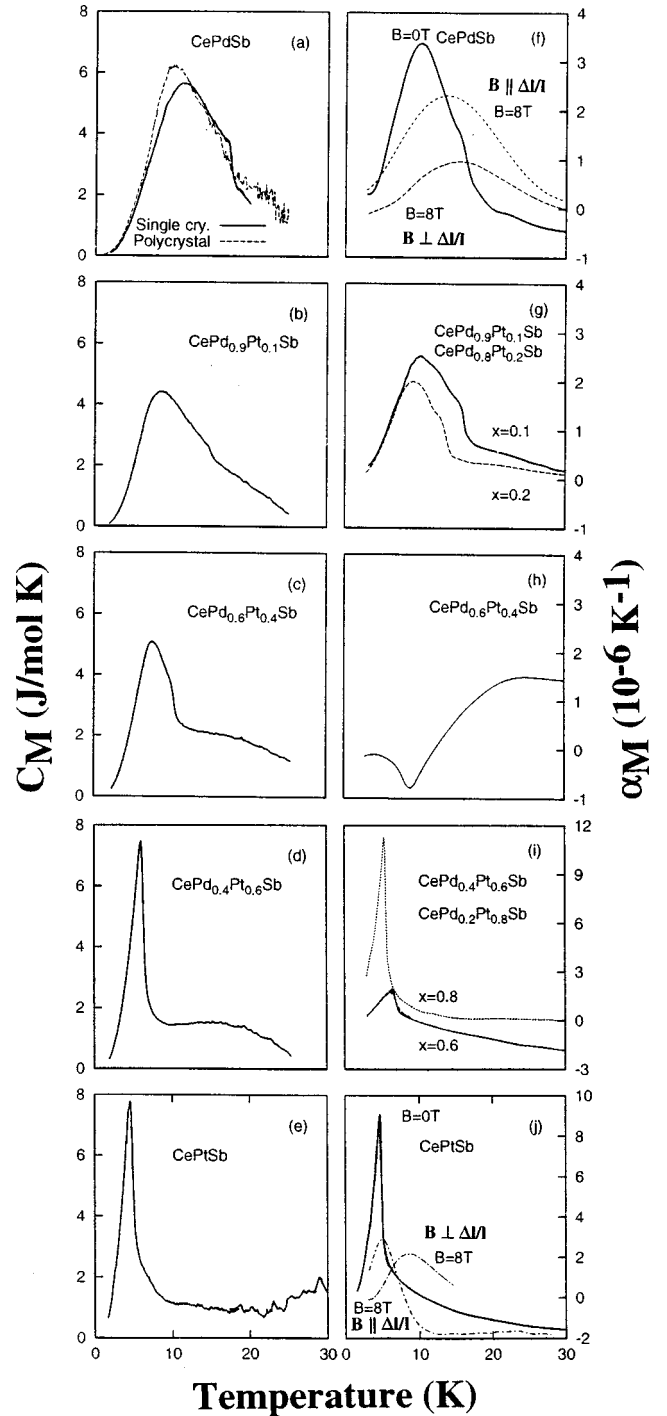


FIG. 4. (a) to (e) the magnetic part of the heat capacity,  $C_M$  and, (f) to (j) the magnetic contribution to the linear thermal expansion,  $\alpha_M$  as a function of temperature for  $\text{CePd}_{1-x}\text{Pt}_x\text{Sb}$  alloys. For  $x = 0$  and 1 alloys  $\alpha_M(T)$  measured in an applied field of 8 T, field parallel and perpendicular to  $\Delta/l$ , is also plotted. The heat-capacity data of CePdSb, polycrystal and single crystal, is from Refs. 12 and 13 and of CePtSb is from Ref. 13.

$\chi'$ , followed by a broad maximum at 8.6 K. In the case of  $x = 0.4$ , the broad peak in  $C_M$  shifts to a lower temperature, 7.44 K and becomes sharper than those of  $x = 0$  and 0.1. The phase diagram (low-dimensional to 3D ordering) obtained as a function of Pt composition from the low-temperature peak position in the heat capacity and  $T_c(\chi_{ac})$  measurements is shown in Fig. 3. This shows that the low-dimensional mag-

netic phase exists for Pt composition,  $x < 0.6$ . The low-temperature heat capacity of substituted alloys could be well explained on the basis of magnon excitation with an energy gap as observed for CePdSb and CePtSb,  $C_M(T) = \gamma T + AT^{1.5} \exp(-\Delta/T)$ . For CePtSb the reported value of  $\gamma$  and  $\Delta$  are 70 mJ/mole-K<sup>2</sup> and 3.83 K, respectively.<sup>14</sup> Further, the reported value of entropy for CePtSb is  $0.76R \ln 2$  at  $T_c = 4.7$  K and  $0.97R \ln 2$  at 6.8 K.<sup>14</sup> Our analysis of the heat-capacity data gave the values of  $\gamma$  (in unit of mJ/mole-K<sup>2</sup>) and  $\Delta$  (in unit of K): 12.2 and 5.83 for  $x = 0.1$ ; 17.1 and 5.32 for  $x = 0.4$ ; and 50.5 and 5.0 for  $x = 0.6$  alloys. These values show that  $\gamma$  increases, while  $\Delta$  decreases with increasing Pt concentration. In the single-ion Kondo model  $\gamma$  is related to the Kondo temperature  $T_K$  by:  $T_K = (N-1)(\pi R/6\gamma)$ , where  $N$  is the degeneracy of the ground state, and  $R$  is the gas constant.<sup>6</sup> This method gives the very high and unphysical value of  $T_K = 396$  K for CePdSb and 62 K for CePtSb, which might suggest that the single-ion Kondo model is not applicable to these compounds, even though the  $T_c$  vs  $P$  curve shows good agreement with Doniach's model.

The magnetic entropy ( $S_m$ ) was calculated by a smooth extrapolation of the  $C_M(T)/T$  curve to zero temperature and integrating with respect to temperature. The estimated value of  $S_m$  (in units of  $R \ln 2$ ) is: 0.3 (at the peak), 0.82 (at  $T_c = 16.05$  K), 0.92 (at 25 K) for  $x = 0.1$ ; 0.37 (at the peak), 0.74 (at  $T_c = 11.72$  K), 0.99 (at 25 K) for  $x = 0.4$ ; and 0.51 (at the peak), 0.95 (at 25 K) for  $x = 0.6$ . These values are consistent with those observed in CePdSb and CePtSb. The observation of full magnetic entropy at 25 K in all the alloys indicates the localized nature of  $4f$  electrons.

### C. Thermal expansion

The magnetic contribution to the coefficient of thermal expansion ( $\alpha_M$ ) of CePd<sub>1-x</sub>Pt<sub>x</sub>Sb alloys in the temperature range below 30 K is shown in Figs. 4(f)–(j). The lattice contribution was subtracted by using  $\alpha(T)$  of nonmagnetic LaPtSb, which showed a typical phonon behavior. The temperature-dependent behavior of  $\alpha_M(T)$  of Ce alloys is almost similar to that observed in the heat capacity, except for alloy  $x = 0.4$ . Also  $\alpha_M(T)$  of  $x = 0.6$  is anomalous compared with the alloys at both ends.  $\alpha_M(T)$  of CePdSb exhibits a weak anomaly at  $T_c$ , which is masked by a broad peak centred at 10 K. The height of the peak of  $\alpha_M$  decreases in  $x = 0.1$  and 0.2 alloys. For the  $x = 0.1$  alloy the peak position in  $\alpha_M(T)$  is slightly higher than that in  $C_M(T)$ . It is to be noted that in the previous study  $\alpha_M(T)$  exhibited an anomaly at  $T_c$  only in the single crystal (along the  $c$  axis), but no clear anomaly was observed in the polycrystalline samples.<sup>15</sup> This suggests that the quality of the present sample is very good. On the other hand  $\alpha_M(T)$  of the  $x = 0.4$  alloy exhibits entirely different behavior from the rest of the alloys: a negative minimum around 9.5 K and a large positive value at 30 K. The temperature at which  $\alpha_M(T)$  exhibits a minimum is slightly higher than the temperature at which  $C_M(T)$  exhibits the peak, but is lower than the  $T_c = 11.7$  K. This anomalous behavior of  $\alpha_M(T)$  would occur if  $dT_c/dP$  had a negative sign for  $x = 0.4$  since  $\alpha_M(T)$  then exhibits a negative peak compared to a positive peak in  $C_M(T)$  because  $dT_c/dP = 3VT_c \Delta \alpha_M / \Delta C_M$ , where  $V$  is molar volume. However, the observed behavior of  $\alpha_M(T)$  of the  $x = 0.4$  alloy is almost

identical to that observed for the single crystal of CePdSb for the  $a$  axis.<sup>15</sup> This may suggest that the  $\alpha_M(T)$  of the  $x = 0.4$  alloy is mainly due to a preferred grain orientation in the polycrystalline sample. In the absence of a pressure study and the single-crystal data of  $\alpha_M(T)$ , it is not possible to confirm the origin of the anomalous behavior of the  $\alpha_M(T)$ . Further  $\alpha_M(T)$  of the  $x = 0.6$  alloy exhibits a broad positive peak, which is wider than that of  $C_M(T)$ , but peaks at the same temperature, and negative values at high temperatures. At higher temperatures  $\alpha_M(T)$  of  $x = 0.6$  alloy exhibits a negative value.  $\alpha_M(T)$  of the  $x = 0.8$  and  $x = 1$  alloys exhibit a very sharp peak at  $T_c$  in agreement with the heat capacity.

A comparison of the heat capacity with the thermal expansion coefficient gives the information about the electronic Grüneisen parameter,  $\Omega_e = 3VB_T \alpha_M / C_M$ , where  $B_T$  is the bulk modulus. The values of  $\alpha_M(T)$  for  $x = 0, 0.1, 0.6$ , and 1.0 alloys at low temperatures (below  $T_c$ ) show good scaling relation with  $C_M(T)$ , using a single-scaling factor. The value of scaling factor, [ $C_M$ (J/mole-K) =  $\alpha_M$ (1/K)  $\times$  scaling factor] is 1.83, 1.75, 4.2 and 0.95 ( $\times 10^6$ ) for  $x = 0, 0.1, 0.6$ , and 1 alloys, respectively. It is to be noted that for the  $x = 0.1$  alloy, due to the peak position being at different temperatures in  $\alpha_M(T)$  and  $C_M(T)$ , the  $\alpha_M(T)$  curve was shifted by  $-1.4$  K in order to obtain the scaling factor. As the value of  $B_T$  is not known for these alloys, a typical value of  $\approx 1$  Mbar was taken for the calculation of  $\Omega_e$ . The estimated value of  $\Omega_e$  is 7.1, 7.5, 3.1, and 13.6 for  $x = 0, 0.1, 0.6$ , and 1 alloys. Except for the  $x = 0.6$  alloy, the values of  $\Omega_e$  are considerably larger than the value 1.3 for the nonmagnetic LaAgGe and 2 for simple metals.<sup>24</sup> Further, the value of  $\Omega_e$  for the  $x = 0.6$  alloy is anomalous among these alloys, but close to the value for normal metal. The value of  $\Omega_e$  for CePdSb has been measured directly from the measurements of the pressure dependent of the Curie temperature  $T_c$  by ac susceptibility measurements.<sup>25</sup> The estimated value is +14, which is consistent with the large value estimated from the heat capacity and thermal expansion coefficient measurements.

In order to investigate the effect of a magnetic field on the  $\alpha_M(T)$  behavior, we have measured  $\alpha_M(T)$  in an applied field of 8 T, applied parallel and perpendicular to the measured-length change,  $\Delta l/l$  for CePdSb and CePtSb. Under a magnetic field the peak becomes broad, its peak value reduced and shifted to a higher temperature. The effect of a magnetic field is larger in the  $B \perp \Delta l/l$  direction than in  $B \parallel \Delta l/l$  direction. This behavior of  $\alpha_M(T)$  is completely consistent with the heat-capacity measurements in an applied field.<sup>14</sup> Further it is to be noted that for CePdSb for the  $B \parallel \Delta l/l$  geometry magnetostriction isotherms measured at various temperatures between 2 K and 30 K exhibit negative value of  $\Delta l/l$ , i.e., length decreases with increasing applied field [Fig. 5(a)]. In the ferromagnetic region (below 9 K), with initial increase in field the  $\Delta l/l$  decreases rapidly with a large slope and then decreases almost linearly with a smaller slope up to 8 T field. The initial decrease in  $\Delta l/l$  with field has been attributed to the removal of domain walls. A very similar behavior in  $\Delta l/l$  with field was also observed for  $B \perp \Delta l/l$  (below 9 K), but in this geometry  $\Delta l/l$  increases with field [Fig. 5(b)] rather than decreases with field as observed in  $B \parallel \Delta l/l$ . An interesting behavior is observed at 9 K for  $B \perp \Delta l/l$ , after sharp increase with fields ( $< 0.3$  T)  $\Delta l/l$

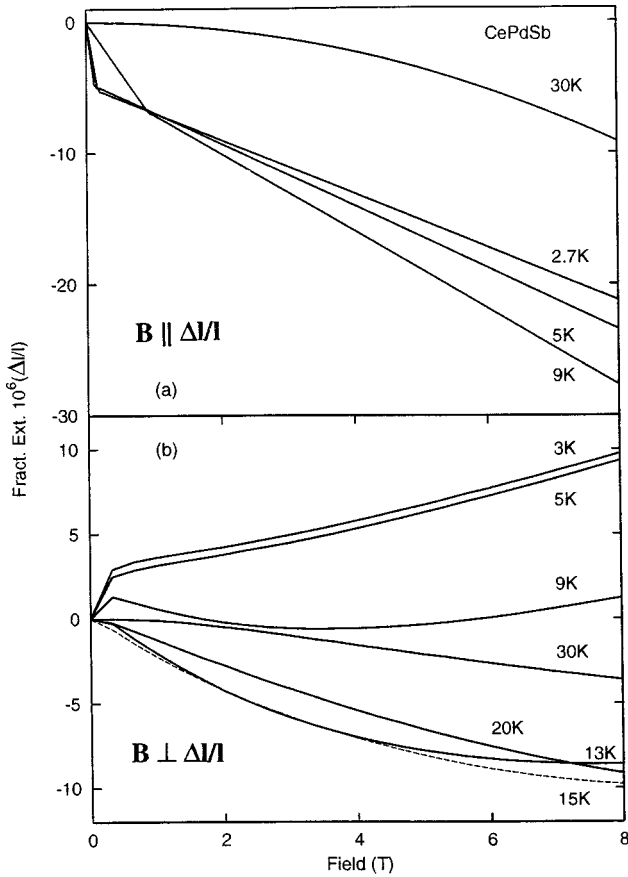


FIG. 5. (a) Parallel ( $B \parallel \Delta l/l$ ) and (b) perpendicular ( $B \perp \Delta l/l$ ) magnetostriction of CePdSb at various temperatures.

decreases with increasing field exhibits a minimum at 3 T, but at 8 T  $\Delta l/l$  has the same value at 0.25 T. It is to be noted that this temperature is very close to the temperature where  $C_M(T)$  and  $\alpha_M(T)$  exhibit anomalous behavior. The absence of the sharp change in  $\Delta l/l$  at the low-fields region above 9 K [see Fig. 5(b)], may suggest that there is no contribution arising from the removal of the domain walls. This may imply that in this temperature range ferromagnetic domains do not exist. This agrees with  $\mu$ SR studies, which show that the damping rate stayed constant with decreasing temperature down to, and through, the onset of ferromagnetic order.<sup>16</sup> For both geometries  $\Delta l/l \propto B^2$  in the paramagnetic region, which is in agreement with the behavior observed for many Ce-based compounds in their paramagnetic state.<sup>23</sup> The  $B^2$  dependence of the magnetostriction could be understood on the basis of the free energy of the system in an applied field, which is given by  $(\lambda M) \cdot B$ , where  $\lambda$  is magnetoelastic coupling constant. For the paramagnetic state  $M \propto B$ , hence free energy and magnetostriction  $\propto B^2$ . If we apply this simple argument in the ferromagnetic state, then the magnetostriction  $\propto B$  at high fields as  $M = M_{\text{sat}} = \text{constant}$  at the high fields. This agrees well with the observed linear behavior of the magnetostriction at high fields below 9 K, but suggests anomalous behavior between 9 K and  $T_c$  for  $B \perp \Delta l/l$ .

#### D. NMR measurements

Figure 6 shows Sb NMR spectra from  $\text{CePd}_{1-x}\text{Pt}_x\text{Sb}$  ( $x=0, 0.2, \text{ and } 1$ ) alloys at low temperatures. The spectra of

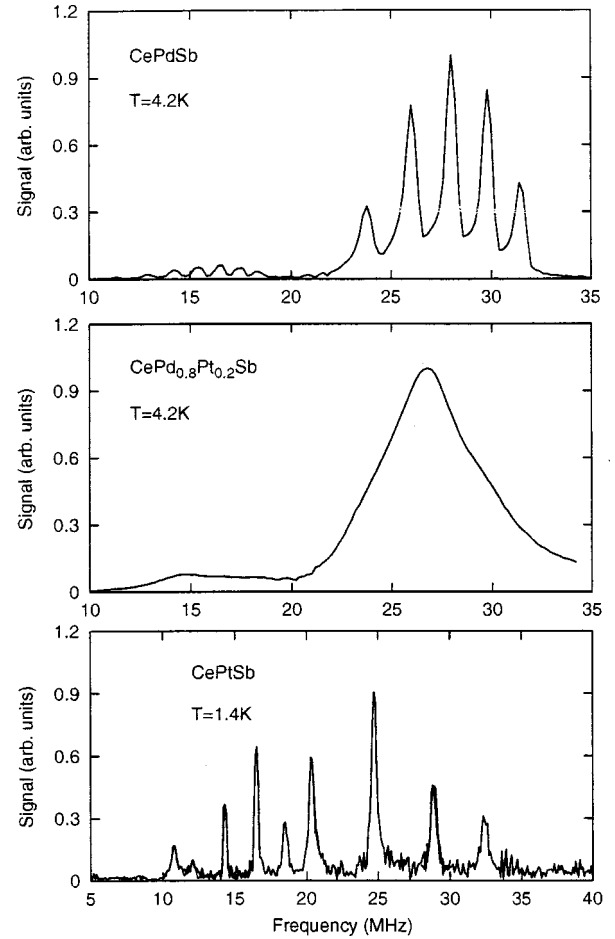


FIG. 6. The Sb NMR spectra from  $\text{CePd}_{1-x}\text{Pt}_x\text{Sb}$  ( $x=0, 0.2$  and  $1$ ) alloys at low temperatures.

$x=0$  and  $x=1$  are well resolved and show the 2I quadrupole-split lines expected from a site of noncubic symmetry. It is clear from the spectra that the quadrupole splitting in CePtSb is stronger than that in CePdSb. On the other hand the spectra of  $x=0.2$ , also of  $x=0.1, 0.4, 0.6, 0.8$  not shown here, show very broad NMR lines without any sign of quadrupole-split lines, centred between 25 MHz and 27.5 MHz. The broad NMR line is due to disorder between Pt and Pd atoms. This leads to a range of quadrupole splittings at the Sb nucleus depending on the number of the nearest-neighbor Pt or Pd atoms. For both CePdSb and CePtSb the sign of the effective field at the Sb nucleus ( $B_{\text{eff}}$ ) was shown to be positive, i.e., parallel to the magnetization, by observing the increase of the NMR frequency in a field of 0.2 T.

In order to analyze the spectrum of CePdSb and CePtSb, it was necessary to go to second order in the expression for the frequency because  $\nu_Q/\nu_0$  was found to be 0.135 (0.15) for  $^{121}\text{Sb}$  ( $^{123}\text{Sb}$ ) in CePdSb and 0.36(0.40) in CePtSb. As the single-crystal magnetization data shows that both compounds have their magnetic moment lying in the  $a$ - $b$  easy plane, we can take the magnetic moment in the ordered state to be at  $90^\circ$  to the electric field gradient. The fits were made separately to  $^{121}\text{Sb}$  and  $^{123}\text{Sb}$  spectra at 4.2 K for CePdSb using the formula from Ref. 26. The calculated values of  $\nu_0$  and  $\nu_Q$  for  $^{121}\text{Sb}$  ( $^{123}\text{Sb}$ ) were 27.77 (15.05) MHz, and 3.80 (2.27) MHz, respectively. The ratio of  $^{121}\text{Sb}/^{123}\text{Sb}$  for  $\nu_0$

( $\nu_Q$ ) is 1.845 (1.67), which is in excellent agreement with the published values for the NMR of Sb 1.847 (1.65).<sup>27</sup>

The lowest frequency satellite lines for CePtSb were not observed, because they were below the working frequency range of our spectrometer, so a complete fit to the spectrum was not possible. The best fit was obtained with the values of  $\nu_0$  and  $\nu_Q$  23.66 (12.82) MHz and 8.5(5.1) MHz for  $^{121}\text{Sb}$  ( $^{123}\text{Sb}$ ), respectively, where the same ratio of  $^{121}\text{Sb}/^{123}\text{Sb}$  for  $\nu_0$  and  $\nu_Q$  was employed as found for CePdSb.

The effective field ( $B_{\text{eff}}$ ) at the Sb nucleus at low temperatures is +2.8 T and +2.3 T for CePdSb and CePtSb, respectively. The small value of  $B_{\text{eff}}$  in CePtSb agrees well with the small value of saturation magnetic moment ( $\mu_s = 0.91\mu_B$ ), compared with ( $\mu_s = 1.32\mu_B$ ) in CePdSb.<sup>14</sup> The factor of two change in the electric field gradient between CePdSb and CePtSb is far larger than would be expected from a point-charge model, Pt-Sb bond length is 2.649 Å in CePtSb compared to the Pd-Sb bond length of 2.679 Å in CePdSb. It must therefore be of electronic origin, most probably arising from the  $d$  band of Pt atoms.

The spontaneous magnetization, estimated from an Arrott plot of the magnetization, of CePdSb exhibits a point of inflexion near 10 K.<sup>16</sup> This agrees with the heat-capacity results as  $C_M$  is proportional to  $dM^2/dT$ . Therefore, it was of interest to compare the temperature dependence of  $B_{\text{eff}}$  determined from zero-field NMR measurements<sup>28</sup> with the magnetization results. However,  $B_{\text{eff}}(T)$  did not show any indication of the anomaly at 10 K and indeed decreases at a slower rate than the spontaneous magnetization.<sup>16</sup> NMR, therefore, shows normal ferromagnetic behavior in CePdSb with  $T_c = 17.5$  K.

#### IV. CONCLUSIONS

In conclusion, we have synthesized  $\text{CePd}_{1-x}\text{Pt}_x\text{Sb}$  ( $0 \leq x \leq 1$ ) alloys and investigated them using XRD, ac susceptibility, heat-capacity, thermal expansion, and zero-field Sb NMR measurements. The heat capacity of the Pd-rich alloys shows a very weak anomaly at  $T_c$ , but a broad peak well below  $T_c$ , which is similar to that observed in CePdSb. The heat capacity of Pt-rich alloys exhibits normal mean-field-type behavior with a sharp peak at  $T_c$ . These results reveal a crossover from the low-dimensional ferromagnetic ordering ( $x \leq 0.4$ ) to normal three-dimensional ( $x \geq 0.6$ ) ferromagnetic ordering with Pt concentration in  $\text{CePd}_{1-x}\text{Pt}_x\text{Sb}$  alloys. The ferromagnetic ordering of CePdSb just below  $T_c$  is characterized by low-dimensional-type ordering, most probably one-dimensional-type ordering of Ce chains along the  $c$  axis, with moments lying in the  $ab$  plane. This has been supported by thermal expansion measurements on a CePdSb single crystal, which shows an anomaly at  $T_c$  only along the  $c$  axis.<sup>15</sup> The real three-dimensional ordering takes places at

low temperatures, i.e., below the broad peak in the heat capacity. From the heat-capacity and ac susceptibility results a phase diagram,  $T$  vs  $x$ , has been constructed, which shows that the low-dimensional magnetic phase exists for  $x < 0.6$  in  $\text{CePd}_{1-x}\text{Pt}_x\text{Sb}$  alloys. The ac susceptibility results reveal that for the Pd-rich alloys the rate of decrease of  $T_c$  with  $x$  is almost 3.5 times that for the Pt-rich alloys. The extrapolated value of a hypothetical  $T_c = 9.1$  K for CePdSb, from the Pt-rich alloys, indicates the real 3D ordering temperature is around 9.1 K in CePdSb, which agrees well with the heat capacity (9.7 K), thermal expansion (10 K), and the results of small angle neutron-scattering measurements (8–12 K). The low-temperature heat-capacity ( $T < T_c$ ) results of all alloys show an energy gap formation in the anisotropic magnon dispersion. The entropy gain at 25 K for all alloys is  $\approx R \ln 2$ , which supports the localized nature of the  $4f$  electrons.

Thermal expansion results agree with the heat-capacity data for the alloys that are either Pd rich or Pt rich. However, the thermal expansion shows anomalous behavior for the alloys with  $x = 0.4$  and 0.6. The estimated value of the electronic Grüneisen parameter for either end of the alloys is very high compared with that of normal metals. The heat capacity along with neutron-scattering measurements ruled out the presence of the Kondo effect in CePdSb. On the other hand, the pressure dependence of the Curie temperature of CePdSb has been explained well with Doniach's model which takes account of the Kondo and RKKY interactions. These results indicate that the presence of the Kondo effect in CePdSb is an open question at present. The magnetostriction measurements on CePdSb also indicated the change in the magnetic state between 9 and 13 K.

Zero-field spin-echo NMR studies show well-defined 2I quadrupole split lines both in CePdSb and CePtSb, confirming the ferromagnetic ground state. The effective field ( $B_{\text{eff}}$ ) at the Sb nucleus at low temperature is +2.8 T and +2.3 T and the quadrupole interaction ( $\nu_Q$ ) for  $^{121}\text{Sb}$  ( $^{123}\text{Sb}$ ) is 3.8 (2.3) MHz and 8.5 (5.1) MHz for CePdSb and CePtSb, respectively. The large value of  $\nu_Q$  in CePtSb cannot be explained simply on the basis of the shorter bond length between Pt-Sb (2.649 Å) in CePtSb and Pd-Sb (2.679 Å) in CePdSb. The factor of two change in the electric field gradient between CePdSb and CePtSb is far larger than would be expected from a point-charge model and must be of electronic origin, most probably arising from the  $d$  band of Pt atoms.

#### ACKNOWLEDGMENTS

We gratefully acknowledge the support of the Engineering and Physical Science Research Council (EPSRC) of the UK. We acknowledge B. D. Rainford for informative discussions.

- <sup>1</sup>D. T. Adroja, S. K. Malik, B. D. Padalia, and R. Vijayaraghavan, Phys. Rev. B **39**, 4831 (1989).
- <sup>2</sup>T. Takabatake, F. Teshima, H. Fujii, S. Nishigori, T. Suzuki, T. Fujita, Y. Yamaguchi, J. Sakurai, and D. Jaccard, Phys. Rev. B **41**, 9607 (1990).
- <sup>3</sup>S. K. Malik and D. T. Adroja, Phys. Rev. B **43**, 6277 (1991).
- <sup>4</sup>S. K. Malik and D. T. Adroja, Phys. Rev. B **43**, 6295 (1991).
- <sup>5</sup>R. Movshovich, J. M. Lawrence, M. F. Hundley, J. Neumeier, J. D. Thompson, A. Lacerda, and Z. Fisk, Phys. Rev. B **53**, 5465 (1996).
- <sup>6</sup>See, for example, E. Bauer, Adv. Phys. **40**, 417 (1991).
- <sup>7</sup>S. Doniach, in *Valence Instabilities and Related Narrow Band Phenomena*, edited by R. D. Parks (Plenum, New York, 1977), p. 169; Physica B **91**, 231 (1977).
- <sup>8</sup>S. K. Dhar, S. K. Malik, and R. Vijayaraghavan, J. Phys. C **14**, L321 (1981); A. L. Cornelius and J. S. Schilling, Phys. Rev. B **49**, 3955 (1994).
- <sup>9</sup>B. D. Rainford and D. T. Adroja, Physica B **194&196**, 365 (1994); B. D. Rainford, D. T. Adroja, A. Neville, and D. Fort, *ibid.* **206&207**, 209 (1995).
- <sup>10</sup>L. Menon and S. K. Malik, Phys. Rev. B **52**, 35 (1995).
- <sup>11</sup>S. K. Malik and D. T. Adroja, J. Magn. Magn. Mater. **102**, 42 (1991).
- <sup>12</sup>O. Trovarelli, J. G. Sereni, G. Schmerber, and J. P. Kappler, Phys. Rev. B **49**, 15 179 (1994).
- <sup>13</sup>K. Katoh, T. Takabatake, A. Ochiai, A. Uesawa, and T. Suzuki, Physica B **230**, 159 (1997); M. Kasaya, H. Suzuki, and K. Katoh, Jpn. J. Appl. Phys., Series **8**, 223 (1993).
- <sup>14</sup>K. Katoh, T. Takabatake, I. Oguro, A. Ochiai, A. Uesawa, and T. Suzuki, J. Phys. Soc. Jpn. **68**, 613 (1999).
- <sup>15</sup>M. J. Thornton, J. G. M. Armitage, R. H. Mitchell, P. C. Riedi, D. T. Adroja, B. D. Rainford, and D. Fort, Phys. Rev. B **54**, 4189 (1996).
- <sup>16</sup>A. J. Neville, B. D. Rainford, D. T. Adroja, and H. Schober, Physica B **223&224**, 271 (1996).
- <sup>17</sup>B. D. Rainford and D. T. Adroja, ILL experimental report, D11 (1998).
- <sup>18</sup>A. L. Cornelius, A. K. Gangopadhyay, and J. S. Schilling, Phys. Rev. B **55**, 14 109 (1997).
- <sup>19</sup>T. Suzuki, Jpn. J. Appl. Phys., Series **8**, 267 (1993).
- <sup>20</sup>J. S. Lord and P. C. Riedi, Meas. Sci. Technol. **6**, 149 (1995).
- <sup>21</sup>R. A. Robinson, A. C. Lawson, K. H. J. Buschow, F. R. Deboer, V. Sechovsky and R. B. Vondreele, J. Magn. Magn. Mater. **98**, 147 (1991).
- <sup>22</sup>L. Menon and S. K. Malik, Phys. Rev. B **55**, 14 100 (1997).
- <sup>23</sup>J. Zieglowaski, H. U. Häfner, and D. Wohlleben, Phys. Rev. Lett. **56**, 193 (1986).
- <sup>24</sup>M. J. Thornton, Ph.D. thesis, St. Andrews University, U.K., 1996.
- <sup>25</sup>P. C. Riedi, J. G. M. Armitage, J. S. Lord, D. T. Adroja, B. D. Rainford, and D. Fort, Physica B **199-200**, 558 (1994).
- <sup>26</sup>G. H. Strauss, J. Chem. Phys. **40**, 1988 (1964).
- <sup>27</sup>R. R. Hewitt and B. F. Williams, Phys. Rev. **129**, 1188 (1963).
- <sup>28</sup>J. S. Lord, G. Tomka, P. C. Riedi, M. J. Thornton, B. D. Rainford, D. T. Adroja, and D. Fort, J. Phys.: Condens. Matter **8**, 5475 (1996).